Universiteit Leiden
The Netherlands

Measurement of the double-layer capacitance of Pt(111) in acidic conditions near the potential of zero charge

Fröhlich, N.L.; Eggebeen, J.J.J.; Koper, M.T.M.

Citation
Fröhlich, N. L., Eggebeen, J. J. J., & Koper, M. T. M. (2024). Measurement of the double-layer capacitance of Pt(111) in acidic conditions near the potential of zero charge. *Electrochimica Acta*, *494*. doi:10.1016/j.electacta.2024.144456

Version: Publisher's Version
License: Creative Commons CC BY 4.0 license
Downloaded from: https://hdl.handle.net/1887/4038342

Note: To cite this publication please use the final published version (if applicable).

Electrochimica Acta 494 (2024) 144456

Contents lists available at ScienceDirect

Electrochimica Acta

journal homepage: www.journals.elsevier.com/electrochimica-acta

Measurement of the double-layer capacitance of Pt(111) in acidic conditions near the potential of zero charge

Nicci L. Fröhlich, Jordy J.J. Eggebeen, Marc T.M. Koper *

Leiden Institute of Chemistry, Leiden University, Einsteinweg 55, 2333 CC Leiden, the Netherlands

ARTICLE INFO

Keywords:
Pt(111)
Double-layer capacitance
Voltammetry
Impedance spectroscopy
AC voltammetry

ABSTRACT

Quantifying the charge density stored at the Pt(111)/aqueous interface using the double-layer capacitance close to the potential of zero charge ($C_{dl,PZC}$) at 0.30 V_{NHE} is of critical importance to elucidating the structure of the electrical double layer (EDL) in the absence of any competing adsorption processes. Marked discrepancies in the values of C_{dl} for this interface exist in the literature, which we show are likely attributable to the measurement technique used. To directly observe the predicted Gouy-Chapman capacitance minimum at the PZC in the double-layer window between 0.40-0.55 V_{RHE}, anomalously low electrolyte concentrations (0.1 mM $HClO_4$) are needed. The measurement of accurate values of $C_{dl,PZC}$ is made highly non-trivial by the extremely large solution resistances (~80-100 kΩ) measured in this required dilute electrolyte as well as the non-negligible deviations from ideal capacitive behaviour (*i.e.*, constant phase element behaviour) displayed even by this well-ordered model electrochemical system. We provide here a comparison between using cyclic voltammetry (CV), electrochemical impedance spectroscopy (EIS), and alternating current-cyclic voltammetry (AC-CV) in determining $C_{dl,PZC}$ for the Pt(111)/$HClO_4$ interface, for different concentrations of the electrolyte. In particular, even when using optimized experimental parameters, we show that the estimated values of $C_{dl,PZC}$ at 0.1 mM $HClO_4$ still display a marked discrepancy depending on the technique used, ranging from 27-41 μF cm^{-2}. At higher $HClO_4$ concentrations, the discrepancies are much less pronounced. Importantly, however, the measured deviation from Gouy-Chapman theory, as quantified by the Parsons-Zobel plot slope, remains consistent across these techniques, implying that the EDL structure of the Pt(111)/aqueous interface continues to prove anomalous and enigmatic.

1. Introduction

Fundamental studies on the electric double layer (EDL) are critical to gaining a better understanding of the arrangement of the ions at the electrode/electrolyte interface, with important ramifications for many electrochemical processes [1,2]. Platinum is one of the most well-studied electrode materials due to its excellent catalytic properties. However, studies on EDL structure remain sparse as Pt(111) is the only basal plane of Pt that exhibits a true "double-layer window" between 0.40-0.55 V_{RHE} [3]. In this potential window, it is widely considered that the Pt(111)/$HClO_4$ interface is ideally polarisable and that there are no additional pseudocapacitive contributions from the dissociation of water into hydrogen and hydroxyl species [4–9], or adsorption from perchlorate anions from the electrolyte [10–13].

To gain a better insight into the structure of the EDL, the charge stored at the electrode/electrolyte interface can be quantified by the so-called (differential) double-layer capacitance, C_{dl} [4,7]. In the absence of specific adsorption, the Gouy-Chapman-Stern (GCS) theory separates the total EDL capacitance, C_{GCS}, into an inner-layer/Stern capacitance, C_i, and diffuse Gouy-Chapman capacitance, C_{GC}: [14–16].

$$\frac{1}{C_{GCS}} = \frac{1}{C_i} + \frac{1}{C_{GC}} \tag{1}$$

GCS theory predicts a minimum in the differential capacitance (C_d) at low electrolyte concentration at the potential of zero charge (PZC, or the potential at which the electrode surface has zero excess electronic (free) charge in contact with a particular electrolyte) in a potential window where no pseudocapacitive/faradaic contributions are expected, as there should only be a (potential-dependent) contribution from C_{GC} [15,17].

Using techniques such as CO displacement [18–20], peroxodisulphate reduction reaction [21], and temperature-induced laser-jump measurements [22,23], it was found that the PZC of Pt(111) lies at 0.30 V_{NHE}. Therefore, on the reversible hydrogen electrode scale, the

* Corresponding author.
E-mail address: m.koper@chem.leidenuniv.nl (M.T.M. Koper).

https://doi.org/10.1016/j.electacta.2024.144456
Received 11 March 2024; Received in revised form 10 May 2024; Accepted 17 May 2024
Available online 24 May 2024
0013-4686/© 2024 The Author(s). Published by Elsevier Ltd. This is an open access article under the CC BY license (http://creativecommons.org/licenses/by/4.0/).

PZC falls within the double-layer window of Pt(111) for pH's 2-4 (PZC = 0.30 + 0.059·pH on the V_{RHE} scale), where a GC-capacitance minimum would be expected. However, it was recently shown that this predicted GC-capacitance minimum is only observable by using extremely dilute electrolyte concentrations of 0.1 mM $HClO_4$ (pH 4), the potential of which (0.54 V_{RHE}) was in excellent agreement with previous PZC studies on Pt(111) [7,24]. The measured capacitance at the PZC ($C_{dl,PZC}$) however, was found to be anomalously high for such dilute electrolytes, which has been rationalised by a weak attractive ion-surface interaction, in turn reducing the Debye length [25]. Schmickler proposed that this anomalously large $C_{dl,PZC}$ actually resulted from a weak specific adsorption of anions in solution [26], however, as $HClO_4$ is widely considered to be a non-specifically adsorbing electrolyte and the trends in $C_{dl,PZC}$ with increasing salt concentrations were found to be independent of the anion identity,[7] we consider chemisorption unlikely the main cause of the anomalous behaviour observed [27].

It has recently been pointed out that there is a marked discrepancy between C_{dl} values obtained for the Pt(111)/$HClO_4$ interface in the literature [28,29], ranging, for example, from 20 μF cm^{-2} in 0.1 M $HClO_4$ (using electrochemical impedance spectroscopy) [4] to 100 μF cm^{-2} in 0.1 mM $HClO_4$ + 5 mM $LiClO_4$ (using cyclic voltammetry) [24]. Although it should be noted that the electrolyte conditions (*i.e.*, ionic strength and pH) for which these values are reported differ significantly, we show in this paper that another main contributor to the discrepancies in the obtained C_{dl} values is likely the used measurement technique.

Two of the most common electrochemical techniques used to obtain C_{dl} have been cyclic voltammetry (CV) and electrochemical impedance spectroscopy (EIS). CV utilises a linear potential ramp, where the corresponding current can be normalised by scan rate in order to obtain the differential capacitance [30]. In EIS, a sinusoidal potential perturbation over a wide frequency range is applied to an electrochemical system assumed to be under steady-state conditions. In the case of the double-layer window of the Pt(111)/$HClO_4$ interface (0.40-0.55 V_{RHE}), the measured impedance is expected to be well-modelled by an electrical equivalent circuit (EEC) consisting of an ideal capacitance (corresponding to the charging of the EDL), in series with a solution resistance [4,31]. Interestingly, a truly ideal capacitance is rarely observed experimentally. Instead, a non-ideal capacitance is observed which can be modelled by a so-called constant phase element (CPE) [32–37].

The origin of CPE behaviour has remained heavily debated in the literature, but has mostly been speculated to arise from a capacitive dispersion across the electrode surface due to electrode roughness [38], adsorption of trace impurities [39], inhomogeneous current/potential distribution due to the disk geometry of the electrode [40–44], or an inherent property of the double-layer itself [45,46]. As we will show, the extremely dilute electrolyte concentrations needed to observe the GC-capacitance minimum actually lead to an increase in CPE behaviour at the PZC. As the CPE has, by definition, a non-linear frequency dependence, there are consequent inherent discrepancies in the differential capacitances obtained using EIS and CV, as the latter technique cannot account for this non-linearity [47].

Alternating current-cyclic voltammetry (AC-CV) has also often been used in obtaining C_{dl}. AC-CV combines both elements of CV and EIS by employing a linear potential ramp upon which a sinusoidally varying wave of a fixed frequency is superimposed [48]. We show here a detailed analysis of how fast Fourier-transform analysis can be used to extract C_{dl} from the fundamental frequency response for the Pt(111)/$HClO_4$ interface near the PZC, discussing the complexities of data processing. Results are then compared to those obtained using EIS and CV to extract the same information, giving a detailed overview of the non-trivial choice of optimal probing parameters required for each of the respective techniques. As we will show, despite the discrepancies in the obtained C_{dl} values, the measured deviation from ideal Gouy-Chapman behaviour was found to be consistent across CV, EIS and AC-CV, as quantified by a Parsons-Zobel plot, suggesting that there continue to remain important unknowns in elucidating the exact EDL structure at the Pt(111)/aqueous interface.

2. Techniques outline

2.1. Cyclic voltammetry (CV)

In cyclic voltammetry (CV), the potential is linearly ramped, where the corresponding current density, j, can be transformed to capacitance, C, by the following relation:

$$j = C\frac{dE}{dt} \tag{2}$$

where $\frac{dE}{dt}$ is the scan rate. The value of C_{dl} at the PZC ($C_{dl,PZC}$) can then be extracted directly from this capacitance curve. Obtaining C_{dl} in this way is only valid under the assumption that there is a negligible time-dependence of the charging of the interface such that all of the obtained current is purely capacitive in nature. Therefore, extracting C_{dl} values is limited to the ideally polarisable double-layer window of Pt (111) in $HClO_4$ electrolyte (0.40-0.55 V) [30]. It should be noted that the extremely dilute electrolyte concentrations that are needed to observe the GC-capacitance minimum (0.1 mM $HClO_4$) lead to significant solution resistances of ~80-100 kΩ [7,24]. Therefore, to reduce the contribution of current, i, to the Ohmic drop (-iR_s) and reduce the resistivity distribution across the electrode, slower scan rates are preferable [30,49,50].

2.2. Electrochemical impedance spectroscopy (EIS)

In electrochemical impedance spectroscopy (EIS), the potential is sinusoidally varied around a mean potential with a certain amplitude, ΔE, which is typically small (between 2-10 mV) such that the response of the system is linear [34,51]. If processes occur on sufficiently different timescales, EIS allows their deconvolution [52]. For Pt(111) in alkaline media, this has proven particularly useful, as the hydrogen adsorption kinetics are sufficiently slow to allow for the double-layer capacitance to be separated from the adsorption capacitance(s). In acidic media, however, the kinetics of hydrogen, hydroxide and anion adsorption are too fast to separate from the double-layer capacitance [4,31,53], such that only a total (*i.e.*, double-layer plus pseudo-) capacitance can be obtained. Therefore, the double-layer window of the Pt(111)/$HClO_4$ interface (0.40 – 0.55 V_{RHE}) is expected to be well-modelled by a simple serial electrical equivalent circuit (EEC) consisting of a resistor and capacitor (RC EEC, SI Fig. 0.1(a)) as there are, in principle, only contributions to the impedance response from the uncompensated solution resistance (resistor, R_s) and the charging of the interface through ion screening (capacitor, C_{dl}) [15].

In reality, the Pt(111)/$HClO_4$ interface actually displays so-called constant phase element (CPE, Q_{dl}) behaviour, such that the serial RQ EEC (SI Fig. 0.1(b)) is needed to model the frequency dispersion exhibited by this system. The impedance of the CPE is given by [54,55]:

$$Z_{CPE} = \frac{1}{Q_{dl}(j\omega)^{\alpha_{dl}}} \tag{3}$$

where α_{dl} is the CPE exponent varying between 0 and 1, where 0 is purely resistive and 1 is purely capacitive, and Q_{dl} is the CPE parameter. Values of $0 < \alpha_{dl} < 1$ indicate a mixed resistive/capacitive process (if $\alpha_{dl} = 0.5$, a Warburg-type element is measured, indicating a diffusion process). If α_{dl} is still relatively close to 1 ($0.8 < \alpha_{dl} < 1$), then this is considered a non-ideal capacitance (*i.e.*, CPE behaviour), which results in a line at an angle of α_{dl} x 90° in the Nyquist impedance representation [52,56].

Several formulae (*e.g.* Brug, Hsu and Mansfeld) have been proposed to convert Q_{dl} to a capacitance as the conversion between these parameters is non-trivial when $\alpha_{dl} \neq 1$ [54–58]. However, as none of these conversion formulae were deemed appropriate in this context due to

non-physical solution-resistance-dependent terms, we show both Q_{dl} and α_{dl} in the following without further conversion to capacitance.

2.3. Alternating current-cyclic voltammetry (AC-CV)

Alternating current-cyclic voltammetry (AC-CV) is a technique that combines both CV and EIS, in principle allowing for a faster method of obtaining the C_{dl} values if appropriate probing parameters are used. However, as we will show, this latter condition is highly non-trivial to satisfy, especially when CPE behavior is present, and complicates the corresponding data analysis [59].

AC-CV employs a linear potential ramp (dc potential scan), whilst simultaneously superimposing an oscillating ac potential wave at a specified frequency, which respectively generate a dc- (equivalent to the CV) and ac-current response. The latter can be deconvoluted from the former by means of a fast Fourier-transform (FFT) analysis. The dc current response information is contained within the 0 Hz band, f_0, regardless of the frequency of the superimposed ac wave, which should be consistent with a normally-obtained CV. Assuming that the double-layer charging is linear in its frequency response, it can be approximated that carrying out AC-CV in the double-layer window of Pt(111) at an appropriate probing frequency should only generate a waveform at the fundamental frequency response, f_1, within which the double-layer charging information should be contained (*i.e.*, the input frequency of the superimposed ac wave) in addition to f_0 [48,52,55]. There should be an absence of higher-order harmonic responses (*i.e.*, f_2, f_3 etc.) which would indicate the presence of non-linear faradaic/pseudocapacitive processes, in turn displaying a frequency-dependent response. By choosing appropriate probing parameters, particularly restricting the amplitude of the oscillation, such higher-order frequency responses can be mitigated as will be further developed later in this manuscript [60,61]. Therefore, if ideal capacitive behavior would hold in the double-layer window, all three techniques (*i.e.*, extracting C from a serial RC EEC in EIS and the C_{dl} values from CV and AC-CV, respectively) should in fact give exactly the same values of C_{dl} [30].

In the linear response approximation, if the potential oscillation varies sinusoidally as a function of time, E(t), with amplitude ΔE, a corresponding sinusoidally varying current response, i(t), will be generated, with amplitude i_0, which will be phase shifted by φ° with respect to the period of the input potential wave just as in EIS:[15,52].

$$\varphi^\circ = \frac{t_{i_{ac,max}} - t_{E_{ac,max}}}{\text{period}} \cdot 360^\circ \tag{4}$$

where $t_{i_{ac,max}}$ and $t_{E_{ac,max}}$ refer to the time at which the maximum in the ac current wave, i(t), and ac potential wave, E(t), occur, respectively [45].

Assuming the angular frequency remains constant and taking the input potential function as the reference with respect to which the current response is defined, phasors (in order to convert between the time and frequency domain) for both the input potential, $\widetilde{E}$, and output current, $\widetilde{i}$, can be defined such that the latter is phase shifted with respect to the former by φ° [52,55]:

$$\widetilde{E} = \Delta E \tag{5}$$

$$\widetilde{i} = i_0 e^{j\varphi^\circ} \tag{6}$$

The impedance, $Z(\omega)$, response can then be described by:[62]

$$Z(\omega) = \frac{\widetilde{E}}{\widetilde{i}} = \frac{\Delta E}{i_0} e^{-j\varphi^\circ} = |Z|(\cos\varphi^\circ + \sin\varphi^\circ) = \mathrm{Re}(Z) + j\mathrm{Im}(Z) \tag{7}$$

$$\mathrm{Re}(Z) = |Z|(\cos\varphi^\circ) = R_s \tag{8}$$

$$\mathrm{Im}(Z) = |Z|(\sin\varphi^\circ) = -\frac{j}{\omega C_{dl,ac}} \tag{9}$$

Therefore, we can extract the double-layer capacitance values of the ac component, $C_{dl,ac}$, as a function of potential from the iFFT-extracted impedance from f_1 to obtain $|Z|$ and by determining the phase shift, φ°, between the period of the input ac potential and the output ac current [45]. It should be noted that Im(Z) here is defined in terms of an ideal capacitor (Eq. 9), so it is assumed that f_1 only contains the purely capacitive C_{dl}-component which is linear in its frequency response, meaning that the non-linear nature of CPE behaviour cannot be appropriately accounted for with this analysis [48].

3. Experimental

The electrochemical glassware cleaning procedure and cyclic voltammetry measurements used in this study were performed following those outlined previously [12]. All the potentials in this manuscript are reported versus the RHE scale.

Potentiostatic electrochemical impedance spectroscopy was carried out at 0.54 V (50 kHz-0.5 Hz, 10 mV) in order to determine the solution resistance, which was then used to maximally compensate the working electrode potential for all electrochemical measurements at 85% *in situ* to avoid potentiostatic oscillation, with the remaining 15% manually compensated post-measurement. The distance between the working and reference electrode (placed in a Luggin capillary) was minimised as far as possible to reduce Ohmic drop. See SI Section 1.2 for detailed explanation of AC-CV Ohmic-drop correction. All potentials reported in this manuscript have been Ohmic drop-corrected accordingly.

Potentiostatic impedance spectra were measured with frequencies ranging from 1 kHz-0.5 Hz (0.1 mM $HClO_4$), or 50 kHz-0.5 Hz (0.1 mM $HClO_4$ + 5 mM $NaClO_4$ and 1 mM $HClO_4$), with varying amplitudes. Blank CVs were taken before and after a series of impedance measurements at 10 mV s^{-1} to ensure that during the time of data acquisition, no significant poisoning, or changes to the electrode surface had occurred.

4. Results and discussion

Here, we provide a detailed analysis of the optimised parameters found for obtaining the double-layer capacitance near the potential of zero charge ($C_{dl,PZC}$) for Pt(111) using cyclic voltammetry (CV), electrochemical impedance spectroscopy (EIS) and alternating current-cyclic voltammetry (AC-CV). We use 0.1 mM $HClO_4$ as a base electrolyte, as we have previously shown that under these conditions a GC-predicted capacitance minimum can be observed that corresponds well with the PZC of Pt(111) measured using other techniques [7,24]. For selected experiments, we add either $NaClO_4$ to increase the ionic strength while keeping pH constant, or use higher concentrations of $HClO_4$.

4.1. Cyclic voltammetry (CV)

Fig. 1 shows the predicted Gouy-Chapman capacitance minimum at the PZC (0.54 V) for Pt(111) in 0.1 mM $HClO_4$ [7,24], corresponding to $C_{dl,PZC}$. For the purely capacitive double-layer window between 0.40-0.55 V for Pt(111), the current density should be directly proportional to the scan rate, v, such that the capacitance values should be equal for all v if we are probing a true double-layer charging process (*i.e.*, $j_c = v \cdot C$) [15].

However, as shown in Fig. 1, a non-trivial scan rate dependence of the values of $C_{dl,PZC}$ is actually observed. The capacitance decreases with v, such that the lowest value of $C_{dl,PZC}$ (32 μF cm^{-2}) is obtained at 2 mV s^{-1}, in close agreement with previously reported values of C_{dl} for Pt (111) [4,31]. Significant increases in $C_{dl,PZC}$ can be observed at higher scan rates, reaching 48 μF cm^{-2} at 20 mV s^{-1}. Interestingly, the $C_{dl,PZC}$ values for greater scan rates (>10 mV s^{-1}) saturate at ~47 μF cm^{-2}, suggesting that a certain threshold of slow scan rates must be reached before seeing a significant drop in the obtained capacitance values. This is unlikely attributable to any artificial currents due to the electronics, or unstable leakage currents arising from the hanging meniscus

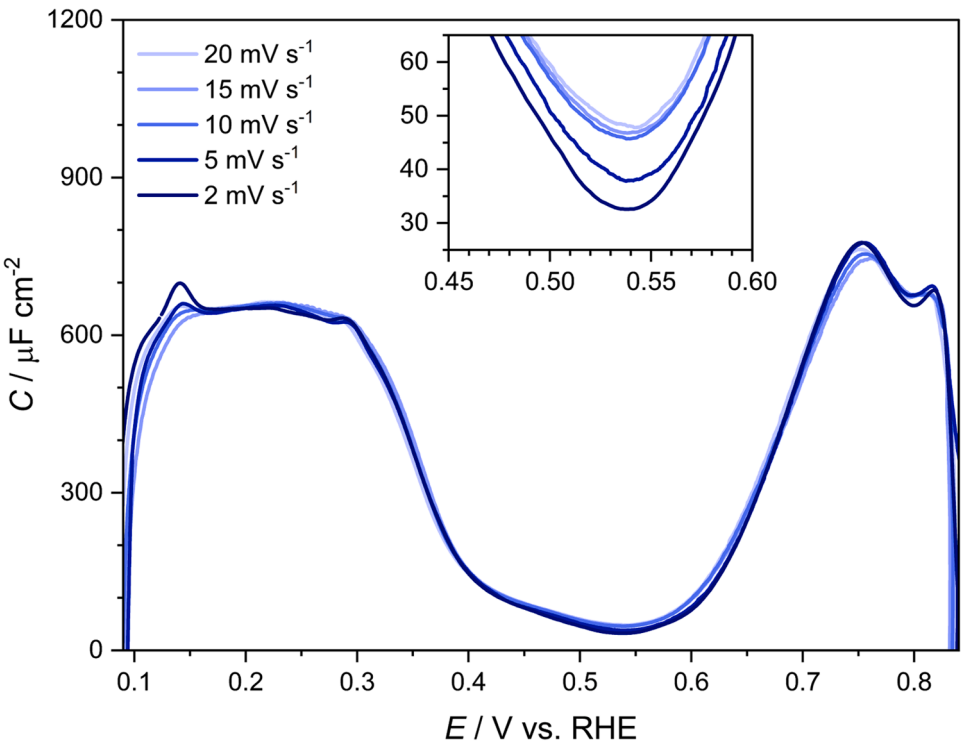

Fig. 1. CVs of Pt(111) in 0.1 mM $HClO_4$ at various scan rates (2-20 mV s^{-1}) when scanning between 0.07-0.85 V. Curve represents the average of positive- and negative-going scans.

configuration, which remains stable for the duration of the measurements [63]. Furthermore, the noise levels were found to be <0.5 nA for all CV measurements, meaning the discrepancies observed in the $C_{dl,PZC}$ as a function of scan rate are not related to different noise levels.

By comparison, the discrepancy in the capacitance values measured as a function of v is significantly less marked in higher conductivity media as shown in Fig. 2 for 1 mM $HClO_4$ (pH 3, $R_s \sim 6$ kΩ, an order of magnitude less than in pH 4).

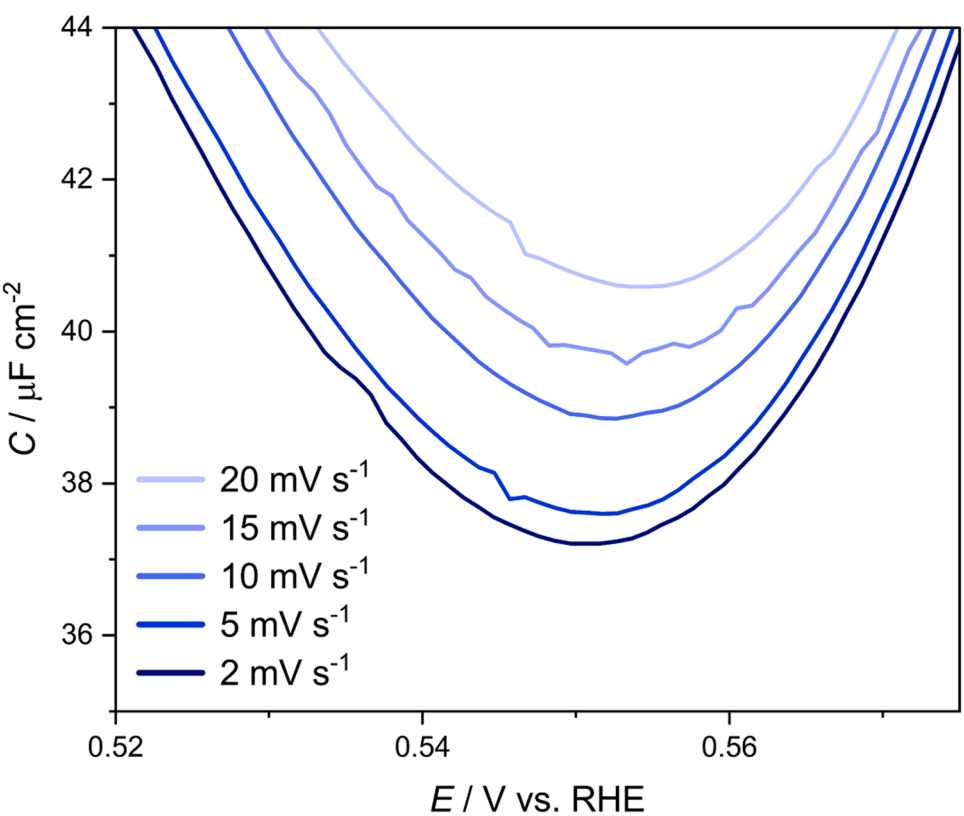

Fig. 2. Zoomed in CVs of Pt(111) in 1 mM $HClO_4$ at various scan rates (2-20 mV s^{-1}) when scanning between 0.07-0.85 V. Curves represent the average of positive- and negative-going scans.

Due to the greater ionic strength in 1 mM $HClO_4$, the inner-layer capacitance starts to dominate [24] meaning that the GC-capacitance minimum at the PZC (0.48 V for pH 3) is no longer directly observable. A capacitance minimum is still observed at ~0.55 V (Fig. 2), however this does not correspond to the predicted GC-capacitance minimum, or the PZC. Instead, this minimum is probably related to a potential dependence of the inner-layer capacitance, or related to pseudocapacitive response due to the onset of hydroxyl adsorption [28]. Arguments as to why the capacitance minimum at pH = 4 (Fig. 1) does correspond to the PZC have been given in our previous papers [7,24]. Therefore, as a value for $C_{dl,PZC}$ cannot directly be obtained in 1 mM $HClO_4$, the values of C in the double layer window will be compared to those in 0.1 mM $HClO_4$ instead. Notably, when increasing v from 2 to 20 mV s^{-1}, C only increases by 4 μF cm^{-2} in 1 mM $HClO_4$ (Fig. 2) compared to 20 μF cm^{-2} in 0.1 mM $HClO_4$ (Fig. 1). Therefore, it is clear that scan rate has a non-trivial impact on the obtained values of $C_{dl,PZC}$ in 0.1 mM $HClO_4$, which is less marked in the case of 1 mM $HClO_4$ electrolyte. The deviation from ideal capacitive behaviour can be attributed to the presence of CPE behaviour, which manifests itself in a non-linear dependency between v and the current measured and, by extension, the capacitance, particularly at low frequencies (scan rates), as will be further developed in Section 4.2 [24,28,30].

4.2. Electrochemical impedance spectroscopy (EIS)

To provide an alternative technique to CV in obtaining the values of $C_{dl,PZC}$, EIS was carried out at the PZC for Pt(111) in 0.1 mM $HClO_4$, the Nyquist impedance plot of which is shown in Fig. 3(a). For comparison with higher conductivity electrolytes, the Nyquist impedance plots obtained in 0.1 mM $HClO_4$ + 5 mM $NaClO_4$ and 1 mM $HClO_4$ at the same potential (0.54 V) are shown in Fig. 3(b) and (c), respectively. The corresponding Nyquist admittance plots are shown in SI Fig. 3.1 for completeness.

In the Nyquist impedance plot representations for each electrolyte (Fig. 3), CPE behaviour is evidenced by the poorer fit of the RC EEC compared to that of RQ. In particular, the extent of CPE behaviour, *i.e.*, the deviation from 90°, is more pronounced in the lower conductivity 0.1 mM $HClO_4$ electrolyte (α_{dl} = 0.95, Fig. 3(a)) compared to the more conductive 0.1 mM $HClO_4$ + 5 mM $NaClO_4$ and 1 mM $HClO_4$ electrolytes (α_{dl} = 0.99 for both, Fig. 3(b,c), respectively). The reduced CPE behaviour exhibited by the more conductive electrolytes is consistent with the results of Lasia *et al.* and is further reflected in the closer agreement between the RQ and RC EEC fits in both the corresponding Nyquist admittance and Bode impedance plots for the higher conductivity electrolytes (0.1 mM $HClO_4$ + 5 mM $NaClO_4$ and 1 mM $HClO_4$, SI Fig. 3.1(b,c); SI Fig. 3.3(b,c) respectively) compared to 0.1 mM $HClO_4$ (SI Fig. 3.1(a); SI Fig. 3.3(a), respectively) [54,52].

In principle, a purely capacitive response should also be independent of the excitation amplitude [56]. As potential perturbation amplitudes that are too small (< 2 mV) can result in a situation where noise will dominate over the signal response from the ac oscillation, EIS measurements with amplitudes between 2-10 mV were carried out in the double-layer window (0.40-0.55 V) of Pt(111) in 0.1 mM $HClO_4$ [51]. However, a clear excitation amplitude dependence can be observed in the obtained values of Q_{dl} and α_{dl} (SI Fig. 3.4), again attributable to the presence of this (non-linear) CPE behaviour. $Q_{dl,PZC}$ values of 40 μF cm^{-2} $s^{(1-\alpha)}$ for an excitation amplitude of 10 mV and 37 μF cm^{-2} $s^{(1-\alpha)}$ for both 2 and 5 mV (SI Fig. 3.4(a)) were obtained, respectively. The values of α_{dl}, however, exhibit the opposite trend with excitation amplitude as α_{dl} increases from 0.946 to 0.954 for excitation amplitudes of 10 to 2 mV (SI Fig. 3.4(b)), respectively, in turn suggesting that increased sensitivity to ideally capacitive processes can be obtained when using smaller excitation amplitudes, consistent with previous literature [34]. Córdoba-Torres *et al.* discussed that there exists an intrinsic coupling between Q_{dl} and α_{dl}, which is also reflected in the non-trivial inverse trends we observe as a function of perturbation amplitude for both Q_{dl} and α_{dl} (SI Fig. 3.4) [64].

Although the values of α_{dl} are reasonably close to 1 in 0.1 mM $HClO_4$, the deviation from ideal capacitive behaviour is significant enough at the PZC, in particular, to be non-negligible. Fig. 4 highlights the discrepancies in the absolute value of C_{dl} that would be obtained by assuming that $Q_{dl} = C_{dl}$ in this potential window, *i.e.*, the differences in the values of Q_{dl} and C_{dl} when fitting with RQ and RC EECs, respectively [65].

The $Q_{dl,PZC}$ value obtained in 0.1 mM $HClO_4$ (37 μF cm^{-2} $s^{(1-\alpha)}$, Fig. 4(a)) is larger than the values of $C_{dl,PZC}$ obtained using CV (32 μF cm^{-2} at 2 mV s^{-1}, Fig. 1) and when fitting with an RC EEC using EIS (34 μF cm^{-2}, Fig. 4(a)). In fact, regardless of the electrolyte, fitting with an RQ EEC will always result in larger Q_{dl} values than the corresponding C_{dl} values from an RC EEC fit due to the contribution of uncompensated α_{dl} (Fig. 4(a)) [54]. Therefore, there will always be a discrepancy between these values. Regardless of the debatable application of currently known conversion formulae between C and Q, Fig. 4 highlights the importance of considering both Q_{dl} and α_{dl} when extracting information about the capacitance as these parameters are intrinsically coupled and should be considered concurrently [64].

Overall, it should be noted that although there is a relatively good agreement between the values of C_{dl} and Q_{dl} obtained from fitting with an RC and RQ EEC, respectively, the discrepancy between these values is greater in the low conductivity 0.1 mM $HClO_4$ (~3 μF cm^{-2}, Fig. 4(a)) compared to the higher conductivity 1 mM $HClO_4$ and 0.1 mM $HClO_4$ + 5 mM $NaClO_4$ electrolytes (~1 μF cm^{-2}, Fig. 4(a)), which must be

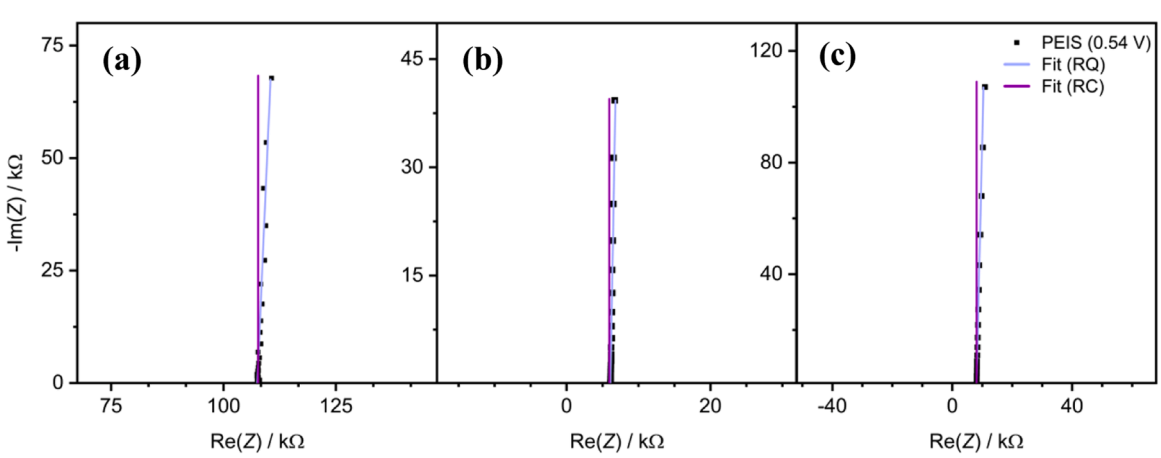

Fig. 3. Nyquist impedance plots of Pt(111) at 0.54 V, ΔE = 5 mV, measured in (a) 0.1 mM $HClO_4$ (1 kHz - 0.5 Hz); (b) 0.1 mM $HClO_4$ + 5 mM $NaClO_4$ (50 kHz - 0.5 Hz); (c) 1 mM $HClO_4$ (50 kHz - 0.5 Hz), with RQ and RC EEC fits shown. See SI Section 3 for explanation of different frequency range used for 0.1 mM $HClO_4$.

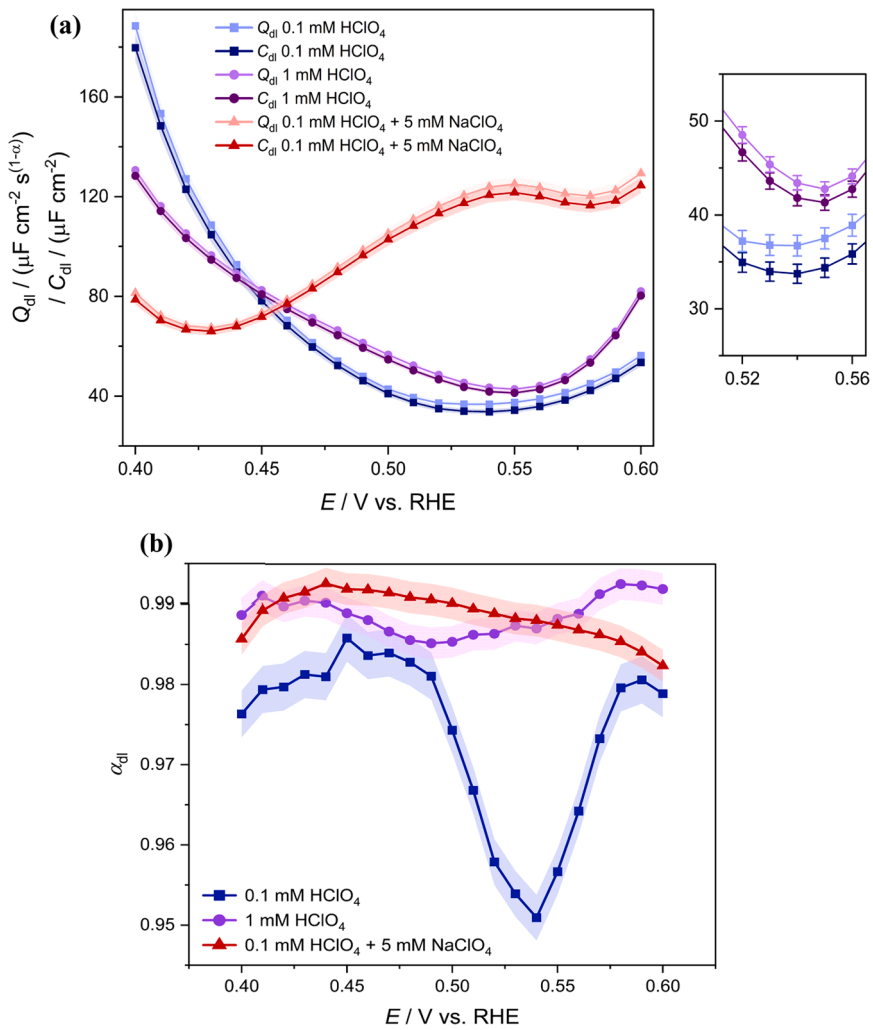

Fig. 4. (a) C_{dl} and Q_{dl} and (b) corresponding α_{dl} values extracted from fitting EIS data of Pt(111) in 0.1 mM $HClO_4$, 0.1 mM $HClO_4$ + 5 mM $NaClO_4$ and 1 mM $HClO_4$ with RC and RQ EECs, respectively, ΔE = 5 mV plotted as a function of potential. Experimental error bars (calculated according to SI Section 1.1) shown as shaded region.

attributable to the (potential-dependent) trends in the observed values of α_{dl} (Fig. 4(b)). The greatest deviation from ideal capacitive behaviour can be observed in 0.1 mM $HClO_4$, which displays a pronounced minimum in α_{dl} of 0.95 at the PZC, whereas at other potentials in the double-layer window, α_{dl} reaches ~0.98 (Fig. 4(b)). Conversely, for both 1 mM $HClO_4$ and 0.1 mM $HClO_4$ + 5 mM $NaClO_4$, α_{dl} remains relatively constant across the potential window, varying only between 0.98-0.99 (Fig. 4(b)). The discrepancy between the values of Q_{dl} and C_{dl}, particularly for 0.1 mM $HClO_4$ (pronounced minimum in α_{dl} at PZC, Fig. 4(b)), can therefore be rationalised in terms of increased deviation of α_{dl} from 1 at the PZC, as an inhomogeneous capacitance distribution across the disc electrode could become magnified without preferential charge polarisation of the electrode, meaning that the non-linear frequency-dependent behaviour (fitted here with a CPE) will become comparatively exacerbated under these conditions [43,44,54,57,65]. Interestingly, in the 1 mM $HClO_4$ (pH 3) electrolyte, the minimum in α_{dl} close to the PZC can still be observed (Fig. 4(b)), while there is no corresponding minimum in the capacitance at this potential (Fig. 4(a)).

These observations once more show the challenges that the low conductivity of the 0.1 mM $HClO_4$ electrolyte presents in terms of obtaining an accurate value of $C_{dl,PZC}$ due to the increased CPE behaviour, such that approximating $Q_{dl} = C_{dl}$ becomes less valid. This has a corresponding influence on the applicability of single-frequency measurements, such as AC-CV, as will be discussed in the subsequent Section 4.3.

4.3. Alternating current-cyclic voltammetry (AC-CV)

In AC-CV, there are three parameters which can be adjusted independently: the scan rate of the dc potential, v, and the amplitude, ΔE, and frequency, f, of the ac potential oscillation. As we will show, these parameters must be selected in careful relation to one another, in part, due to the non-negligible presence of CPE behaviour particularly at the PZC as evidenced by EIS (Section 4.2, Fig. 4(b)). This CPE is, by definition, non-linear in its frequency response, undermining the required assumption that the capacitance behaves ideally (just as for CV) to extract C_{dl} values. In particular, the choice of probing frequency also becomes significantly more complicated as AC-CV only utilizes a singular excitation frequency such that the frequency dispersion inherent to the system cannot be accounted for. Nonetheless, the relatively close fit of the serial RC EEC using EIS (Section 4.2) leads us to investigate the appropriateness of AC-CV in extracting an accurate $C_{dl,PZC}$ value in this system, even in the presence of this CPE behaviour. We provide here a summary of the optimized parameters and their selection; a more detailed explanation can be found in SI Section 4.

To choose appropriate AC-CV probing frequencies, the EIS Bode impedance plots (SI Fig. 3.3) were considered. In the case of a serial RC/RQ EEC, the impedance response becomes dominated by R_s at higher

probing frequencies, resulting in a phase angle of close to 0°. At lower frequencies, the capacitive element will contribute more and eventually dominate over the response of R_s, leading to a phase angle of (close to) -90°. The frequency at which this phase angle change will occur is dependent on R_s, as a larger R_s results in a shift along the Re(Z) axis, such that for 0.1 mM $HClO_4$, the impedance response only becomes mostly dominated by the capacitive element at frequencies below ~10 Hz (SI Fig. 3.3(a)) [55]. Therefore, superimposed frequencies of 5, 10 and 20 Hz were chosen to obtain AC-CV capacitance curves.

Previous literature has alluded to a so-called "slow-scan limit approximation" to ensure reliable AC-CV measurements, such that $\Delta E^*\omega >> \nu$, where ω is the angular frequency ($\omega = 2\pi f$) [66]. Although rather generalized, this relation ensures that, over the period of multiple oscillations, the dc potential changes significantly less than the amplitude of the ac potential modulation, such that both f and ΔE need to be significantly larger than ν. As discussed preciously, $\nu = 2$ mV s^{-1} was considered to be acceptably fast enough to prevent unnecessarily long experimental times, in turn mitigating the effects of meniscus evaporation and eventual changes in Ohmic drop and the edge effect contribution of the disc electrode [67,68]. Following the "slow-scan limit approximation", ΔE was therefore chosen to be 10 mV such that $f^*\Delta E >$ 314 mV s^{-1} $>> \nu = 2$ mV s^{-1} at $f = 5$ Hz. It is also important that ΔE is small enough to ignore the effect of non-linear responses as in EIS [34,51].

Using these selected parameters, a representative power spectrum obtained from FFT analysis of an AC-CV scan in the double-layer window (0.40-0.55 V) of Pt(111) in 0.1 mM $HClO_4$ with $f = 5$ Hz, $\Delta E = 10$ mV and $\nu = 2$ mV s^{-1} (SI Fig. 4.1) reveals that the main frequency signal responses can be observed at 5 Hz (fundamental frequency response, f_1) and 0 Hz (dc potential wave, f_0, corresponding to the normally-obtained CV when inverse Fourier-transformed). The lack of higher-order harmonics indicates the absence of non-linear capacitive charging processes, which is expected for the double-layer window (0.40-0.55 V) and suggests that the selected AC-CV parameters in this case are indeed appropriate for probing this system [48,61].

To elucidate the effect of probing frequency, AC-CV was carried out for Pt(111) in 0.1 mM and 1 mM $HClO_4$ at f = 5/10/20 Hz and the corresponding phase angles were compared to those derived from the EIS Bode plot at the same frequencies (SI Fig. 4.2 and 4.5 for 0.1 mM and 1 mM $HClO_4$, respectively). The phase angles obtained using AC-CV and EIS were found to differ markedly. In fact, using a probing frequency of f = 20 Hz in 0.1 mM $HClO_4$ resulted in entirely positive phase angles (SI Fig. 4.2(a)), leading to a non-physical negative capacitance curve (SI Fig 4.3). As is explained in more detail in SI Section 4, this relates to the main limitation of AC-CV, where, depending on the choice of parameters, by simultaneously scanning the potential and superimposing an oscillating perturbation, the system does not have sufficient time to reach a steady response to the probing frequency at a certain potential. This lack of equilibration time leads to an exacerbated lag between the input ac potential wave and the output ac current wave when initially starting the AC-CV scan, resulting in larger phase angles than expected, particularly for greater probing frequencies and higher solution resistances. In a sense, the initial phase angle measured for an AC-CV scan in our system can be seen as a measure of how out of sync the initial potential perturbation is with that of the output ac current, convoluting the true phase angle response inherent to the impedance of the system. We therefore suggest that EIS, in this context, should serve as the standard by which appropriate probing parameters should be selected for AC-CV measurement, at least in the absence of appropriate hardware (*e.g.* lock-in amplifier), which can measure the measurement-induced "lag" between E(t) and i(t). That is to say, a close agreement between the phase angles derived by both AC-CV and EIS should be observed in order to select appropriate probing parameters.

Hence, as the initial phase angles derived from EIS and AC-CV at the start of the scan are most consistent with each other for $f_1 = 5$ Hz for 0.1 mM $HClO_4$ (SI Fig. 4.2) and $f_1 = 20$ Hz for 1 mM $HClO_4$ (SI Fig. 4.5), respectively, these probing frequencies were considered to be the most accurate when $\nu = 2$ mV s^{-1} and $\Delta E = 10$ mV. Therefore, for simplicity, we show here a summary of the main results using these optimal probing parameters. As outlined in Eq. 9, the phase angles (SI Fig. 4.11) and $|Z|$ (SI Fig. 4.12) need to be considered in turn in order to derive the ac-capacitance values. The corresponding phase angles obtained for both 0.1 mM (SI Fig. 4.11(a)) and 1 mM $HClO_4$ (SI Fig. 4.11(b)) in the H_{upd} and OH_{ads} regions are relatively consistent between AC-CV and EIS (derived from EIS Bode plots, SI Fig. 3.3), remaining close to 0° in both cases, as is expected for the large capacitance measured in the presence of pseudocapacitive processes. On the other hand, the significantly lower capacitance measured in the double-layer window (0.40-0.55 V) results in correspondingly larger phase angles (SI Fig. 4.11) as according to:

$$\varphi = \tan^{-1}\left(-\frac{1}{\omega C_{dl} R_s}\right) \tag{10}$$

However, there is a marked discrepancy in the phase angles obtained using AC-CV and EIS in the double-layer window for both electrolytes, differing by ~35° and ~45° for 0.1 mM and 1 mM $HClO_4$, respectively, where the AC-CV-derived phase angles are always larger than those obtained using EIS. To some extent, the increased CPE behaviour at the PZC (Section 4.2), could explain the discrepancy between the AC-CV-obtained phase angle compared to EIS due to the assumption of ideal capacitive behaviour made in the former analysis.

Despite the discrepancy between the absolute values of the phase angles derived from AC-CV compared to EIS in the double-layer window (SI Fig. 4.11), the corresponding AC-CV capacitance curves using the optimised probing parameters for 0.1 mM and 1 mM $HClO_4$ are shown in Fig. 5.

The value of $C_{dl,PZC}$ in 0.1 mM $HClO_4$ is lower than the value of $C_{dl,min}$ in 1 mM $HClO_4$ by ~6 μF cm^{-2} (Fig. 5), which is in relatively close agreement with the difference obtained using CV between these electrolytes (5 μF cm^{-2}, Section 4.1). However, the absolute value of $C_{dl,PZC}$ is ~8 μF cm^{-2} greater than that measured using CV (ν = 2 mV s^{-1}), which could be attributed to a non-trivial dependence on the AC-CV probing parameters such that the extracted ac- capacitance value becomes somewhat arbitrary, particularly due to the high solution resistance and presence of CPE behaviour in this system. The use of AC-CV as a stand-alone measurement technique also becomes rather redundant in this context due to the heavy reliance on EIS to find appropriate probing parameters.

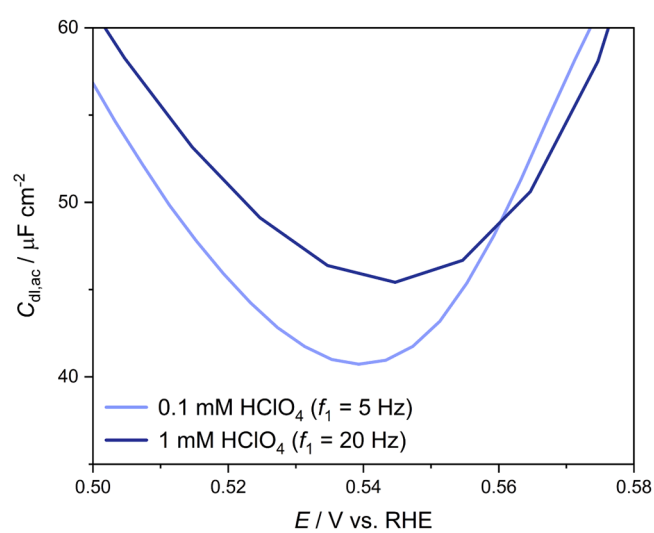

Fig. 5. Capacitance curves extracted from iFFT of the fundamental frequency response, f_1, of the positive-going scan (0.07-0.85 V) for Pt(111) measured in 0.1 mM $HClO_4$ at $f = 5$ Hz and 1 mM $HClO_4$ at $f = 20$ Hz, respectively ($\Delta E = 10$ mV, $\nu = 2$ mV s^{-1}).

However, as discussed in the AC-CV method Section 2.3, the 0 Hz waveform in the FFT power plot (f_0) can be inverse Fourier-transformed to obtain the dc current response and normalized by scan rate to obtain the capacitance just as for a normally-obtained CV [48]. The resulting AC-CV-obtained dc capacitance curves in 0.1 mM and 1 mM $HClO_4$ electrolytes are compared to the corresponding normally-obtained CV capacitance curves at 2 mV s^{-1} in SI Fig. 4.13. The dc-obtained AC-CV capacitances are frequency-independent for $f = 5/10/20$ Hz as expected for both electrolytes as, in principle, the superimposed sinusoidal perturbation should have no effect on the dc current response. However, a consistently lower capacitance of ~8 μF cm^{-2} is obtained for the dc-component obtained using AC-CV compared to CV in 0.1 mM $HClO_4$ (SI Fig. 4.13(a)), which is also observed in 1 mM $HClO_4$ (~4 μF cm^{-2}, SI Fig. 4.13(b)).

4.4. Technique comparison summary

As can be seen in Fig. 6, there are clear discrepancies between the obtained values of $C_{dl,PZC}$ for Pt(111) in 0.1 mM $HClO_4$ depending on the measurement technique (CV, EIS, or AC-CV) even when optimal probing parameters are used, ranging from 27 to 41 μF cm^{-2}. By comparison, the discrepancies in the capacitance values obtained in the double-layer window were found to be less marked for 1 mM $HClO_4$ (SI Fig. 5.1).

Interestingly, the lowest value of $C_{dl,PZC}$ (27 μF cm^{-2}) was measured from the dc-component of AC-CV. The higher values of $C_{dl,PZC}$ obtained from the ac-component of AC-CV and EIS (34-41 μF cm^{-2}) compared to CV (32 μF cm^{-2}) can be attributed to the presence of CPE behaviour, in turn resulting in a non-linear frequency dependence and a non-trivial relationship to an ideal capacitance.

A Parsons-Zobel plot can be used to quantify the deviation of the differential capacitance from ideal Gouy-Chapman behaviour, where the inverse of the calculated Gouy-Chapman capacitance is plotted versus the inverse of the measured differential capacitance at the PZC ($C_{dl,PZC}$). According to Gouy-Chapman-Stern theory, this slope should be 1, however, our group has previously reported a slope of ca. 0.035 for Pt (111) [7,24]. The lower slope was thought unlikely to be the result of any specific adsorption/chemisorption effects due to the lack of specific (anion) effects, but rather a near-surface accumulation effect [26,27]. Using the optimised parameters discussed in the above sections, Fig. 7 compares the PZ-plots obtained using CV, EIS and AC-CV for 0.1 mM $HClO_4 + x$ mM $NaClO_4$.

Fig. 7 shows that, regardless of the limitations of each technique in terms of extracting accurate values for $C_{dl,PZC}$, a similar PZ-plot slope can be observed between the three techniques, suggesting that using appropriate probing parameters for each technique still allows for consistency between obtained $C_{dl,PZC}$ values. Importantly, the PZ-plot slope is significantly less than 1 for all techniques, consistent with previous publications [7,24], albeit that the average slope across the three techniques (0.046) is slightly greater than previously reported, which can be attributed to the lower values of $C_{dl,PZC}$ measured with the optimised parameters for each measurement technique.

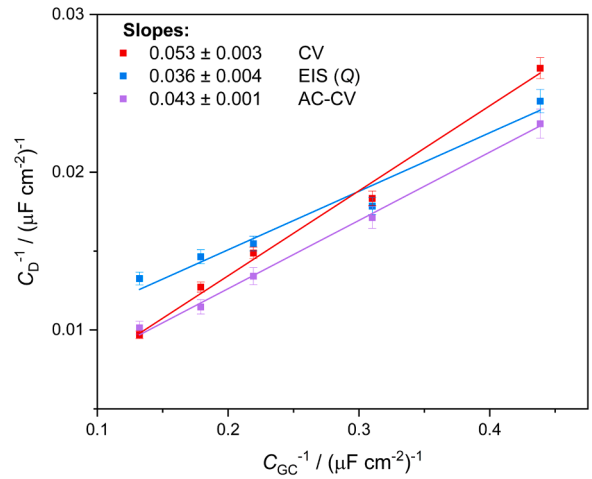

Fig. 7. Parsons-Zobel plot for Pt(111) in 0.1 mM $HClO_4 + x$ mM $NaClO_4$ for the double-layer capacitance obtained at the PZC (0.54 V) from CV (2 mV s^{-1}); EIS (1 kHz-0.5 Hz, 5 mV) for Q when fitting with an RQ EEC; and $C_{dl,ac,PZC}$ extracted from iFFT of the fundamental frequency response, f_1, of the positive-going scan (0.07-0.85 V) of AC-CV ($v = 2$ mV s^{-1}, $f = 5$ Hz, $\Delta E = 10$ mV). Experimental error bars obtained according to SI Section 1.1.

5. Conclusion

In conclusion, we have shown that determining the C_{dl} near the PZC for Pt(111) in acidic media is challenging, mainly due to the extremely low electrolyte concentrations that are needed to observe the Gouy-Chapman-predicted capacitance minimum. We provide a comparison between using CV, EIS and AC-CV as techniques to determine $C_{dl,PZC}$ for the Pt(111)/0.1 mM $HClO_4$ interface, giving a detailed analysis of which parameters should be used to optimally probe the electrochemical system.

From the above discussions, it is clear that all three techniques have their respective disadvantages in the context of obtaining an accurate

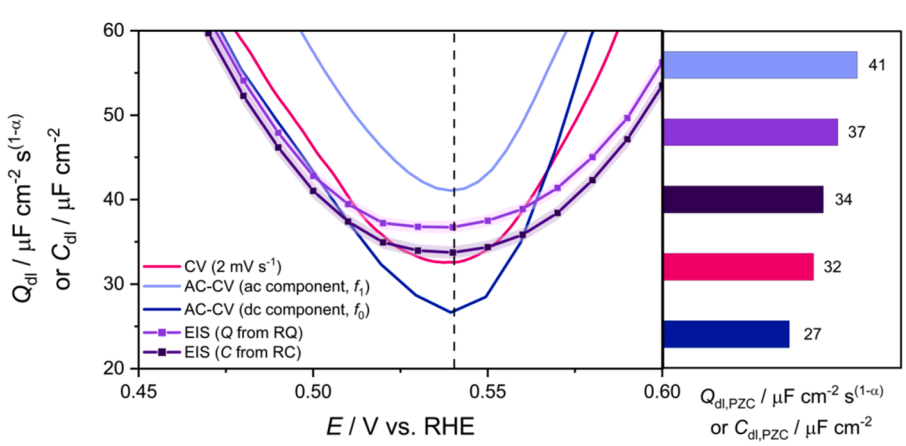

Fig. 6. Comparison of capacitance values obtained for Pt(111) in 0.1 mM $HClO_4$ using CV (2 mV s^{-1}), curves represent the average of positive- and negative-going scans; EIS (1 kHz-0.5 Hz, 5 mV) for C and Q when fitting with an RC and RQ EEC, respectively with experimental error bars (calculated according to SI Section 1.1) shown as shaded region; capacitance curves extracted from iFFT of the fundamental frequency response, f_1, of the positive-going scan of AC-CV ($v = 2$ mV s^{-1}, $f = 20$ Hz, $\Delta E = 10$ mV, 0.07-0.85 V) with no phase angle correction and the corresponding dc component extracted from f_0 represented as capacitance curves (left) and corresponding $C_{dl,PZC}$ values (right).

value of $C_{dl,PZC}$ under these conditions. Both CV and AC-CV suffer from the disadvantage that they rely on dynamically scanning the potential as a function of time, impinging on the linearity and frequency (or scan-rate) independence of the double-layer charging response. EIS, on the other hand, is measured under steady-state conditions, such that time is allowed for equilibration to the applied potential when small excitation amplitudes (<10 mV) are used. In particular, it was found that the Pt (111)/0.1 mM $HClO_4$ interface exhibits CPE behaviour, introducing a non-linear frequency dependence that significantly complicates analysis. This CPE behaviour is likely attributable to the capacitance dispersion that arises from the inhomogeneous current distribution due to the hanging meniscus configuration with which these EIS measurements were carried out, which could, theoretically, be mitigated using a recessed electrode [69].

EIS is the only technique of the three that is able to fit the observed frequency dispersion in its entirety across a wide range of frequencies, however, extracting a capacitance value from the obtained Q_{dl} parameter is non-trivial and leads to discrepancies in the values due to an intrinsic coupling to the CPE exponent, α_{dl}, particularly due to there being a pronounced non-ideal capacitive behaviour at the PZC (*i.e.*, minimum in α_{dl}) and at lower frequencies. This non-linear frequency-dependence introduces significant challenges in finding appropriate probing parameters for single frequency measurement techniques such as AC-CV, in particular, and the consequent processing required as the choice of probing frequency becomes critical to the obtained capacitance value. In fact, in 0.1 mM $HClO_4$, it was found that a probing frequency of 5 Hz ($\Delta E = 10$ mV, $\nu = 2$ mV s^{-1}) was the most reliable in terms of extracting accurate $C_{dl,PZC}$ values. However, it is our opinion that the choice of appropriate experimental parameters for AC-CV must be done in tandem with a high-frequency processing hardware such as EIS (or a lock-in amplifier), meaning that AC-CV cannot be used as a stand-alone technique in this context.

Regardless of the individual limitations that each technique poses, a relatively consistent Parsons-Zobel plot slope of ~0.046 was obtained, showing that the Pt(111)/$HClO_4$ interface still exhibits highly non-trivial deviations from ideal Gouy-Chapman behaviour and continues to highlight the many unknowns of this EDL structure, even in this model system.

CRediT authorship contribution statement

Nicci L. Fröhlich: Writing – review & editing, Writing – original draft, Methodology, Investigation, Formal analysis, Data curation, Conceptualization. **Jordy J.J. Eggebeen:** Writing – review & editing, Methodology, Investigation, Formal analysis, Data curation, Conceptualization. **Marc T.M. Koper:** Writing – review & editing, Supervision, Funding acquisition, Formal analysis, Conceptualization.

Declaration of competing interest

The authors declare that they have no known competing financial interests or personal relationships that could have appeared to influence the work reported in this paper.

Data availability

Data will be made available on request.

Acknowledgements

This work was supported by the European Research Council (ERC), Advanced Grant no. 101019998 “FRUMKIN”.

Supplementary materials

Supplementary material associated with this article can be found, in the online version, at doi:10.1016/j.electacta.2024.144456.

References

[1] O.M. Magnussen, A. Groß, Toward an atomic-scale understanding of electrochemical interface structure and dynamics, J. Am. Chem. Soc. 141 (2019) 4777–4790.
[2] S.J. Shin, et al., On the importance of the electric double layer structure in aqueous electrocatalysis, Nat. Commun. 13 (2022) 174.
[3] M.T.M. Koper, Blank voltammetry of hexagonal surfaces of Pt-group metal electrodes: comparison to density functional theory calculations and ultra-high vacuum experiments on water dissociation, Electrochim. Acta 56 (2011) 10645–10651.
[4] T. Pajkossy, D.M. Kolb, Double layer capacitance of Pt(111) single crystal electrodes, Electrochim. Acta 46 (2001) 3063–3071.
[5] R. Rizo, E. Herrero, V. Climent, Juan.M. Feliu, On the nature of adsorbed species on platinum single crystal electrodes, Curr. Opin. Electrochem. 38 (2023) 101240.
[6] A. Berná, V. Climent, J.M Feliu, New understanding of the nature of OH adsorption on Pt(111) electrodes, Electrochem. Commun. 9 (2007) 2789–2794.
[7] K. Ojha, K. Doblhoff-Dier, M.T.M. Koper, Double-layer structure of the Pt(111)–aqueous electrolyte interface, Proc. Natl. Acad. Sci. USA 119 (2022) e2116016119.
[8] M.J. Kolb, F. Calle-Vallejo, L.B.F. Juurlink, M.T.M Koper, Density functional theory study of adsorption of H2O, H, O, and OH on stepped platinum surfaces, J. Chem. Phys. 140 (2014) 134708.
[9] M. Schalenbach, Y.E. Durmus, H. Tempel, H. Kungl, R.A. Eichel, The role of the double layer for the pseudocapacitance of the hydrogen adsorption on platinum, Sci. Rep. 12 (2022) 3375.
[10] J.J. Calvante, N.S. Marinković, Z. Kováčová, W. Ronald Fawcett, SNIFTIRS studies of the double layer at the metal/solution interface. Part 1. Single crystal gold electrodes in aqueous perchloric acid, J. Electroanal. Chem. 421 (1997) 49–57.
[11] K.A. Jaaf-Golze, D.M. Kolb, D. Scherson, On the voltammetry of curves of Pt (111) in aqueous solutions, J. Electroanal. Chem. Interfacial Electrochem. 200 (1986) 353–362.
[12] N. Fröhlich, et al., Effect of trace impurities in perchloric acid on blank voltammetry of Pt(111), Electrochim. Acta 466 (2023) 143035.
[13] J. Mostany, E. Herrero, J.M. Feliu, J. Lipkowski, Determination of the Gibbs excess of H and OH adsorbed at a Pt(111) electrode surface using a thermodynamic method, J. Electroanal. Chem. 558 (2003) 19–24.
[14] W. Schmickler, E Santos, Interfacial Electrochemistry, Springer, 2010.
[15] A.J. Bard, L.R. Faulkner, Electrochemical Methods Fundamentals and Applications, John Wiley & Sons, Inc., 2001.
[16] D.C. Grahame, The electrical double layer and the theory of electrocapillarity, Chem. Rev. 41 (1947) 441–501.
[17] A.N. Frumkin, O.A. Petrii, Potentials of zero total and zero free charge of platinum group metals, Electrochim. Acta 20 (1975) 347–359.
[18] M.J. Weaver, Potentials of zero charge for platinum(111)−aqueous interfaces: a combined assessment from in-situ and ultrahigh-vacuum measurements, Langmuir. 14 (1998) 3932–3936.
[19] J.M. Feliu, J.M. Orts, R. Gómez, A. Aldaz, J. Clavilier, New information on the unusual adsorption states of Pt(111) in sulphuric acid solutions from potentiostatic adsorbate replacement by CO, J. Electroanal. Chem. 372 (1994) 265–268.
[20] J. Clavilier, et al., Study of the charge displacement at constant potential during CO adsorption on Pt(110) and Pt(111) electrodes in contact with a perchloric acid solution, J. Electroanal. Chem. 330 (1992) 489–497.
[21] R. Martínez-Hincapié, V. Climent, J.M. Feliu, Peroxodisulfate reduction as a probe to interfacial charge, Electrochem. Commun. 88 (2018) 43–46.
[22] P. Sebastián, R. Martínez-Hincapié, V. Climent, J.M. Feliu, Study of the Pt (111) | electrolyte interface in the region close to neutral pH solutions by the laser induced temperature jump technique, Electrochim. Acta 228 (2017) 667–676.
[23] V. Climent, B.A. Coles, R.G. Compton, Coulostatic potential transients induced by laser heating of a Pt(111) single-crystal electrode in aqueous acid solutions. rate of hydrogen adsorption and potential of maximum entropy, J. Phys. Chem. B 106 (2002) 5988–5996.
[24] K. Ojha, N. Arulmozhi, D. Aranzales, M.T.M. Koper, Double Layer at the Pt(111)–aqueous electrolyte interface: potential of zero charge and anomalous gouy–chapman screening, Angew. Chem. Int. Ed. 59 (2020) 711–715.
[25] K. Doblhoff-Dier, M.T.M. Koper, Electric double layer of Pt(111): known unknowns and unknown knowns, Curr. Opin. Electrochem. 39 (2023) 101258.
[26] W. Schmickler, The effect of weak adsorption on the double layer capacitance, ChemElectroChem 8 (2021) 4218–4222.
[27] K. Doblhoff-Dier, M.T.M Koper, Modeling the Gouy–Chapman diffuse capacitance with attractive ion–surface interaction, J. Phys. Chem. C 125 (2021) 16664–16673.
[28] L. Zhang, J. Huang, Measurement and interpretation of the double layer capacitance of Pt(111)/aqueous solution interfaces, Curr. Opin. Electrochem. 42 (2023) 101419.
[29] J. Huang, Zooming into the Inner Helmholtz Plane of Pt(111)–aqueous solution interfaces: chemisorbed water and partially charged ions, JACS Au 3 (2023) 550–564.
[30] D.M. Morales, M. Risch, Seven steps to reliable cyclic voltammetry measurements for the determination of double layer capacitance, J. Phys.: Energy 3 (2021) 34013.

[31] K.J.P. Schouten, M.J.T.C. van der Niet, M.T.M Koper, Impedance spectroscopy of H and OH adsorption on stepped single-crystal platinum electrodes in alkaline and acidic media, Phys. Chem. Chem. Phys. 12 (2010) 15217–15224.
[32] J. Tymoczko, W. Schuhmann, A.S. Bandarenka, The constant phase element reveals 2D phase transitions in adsorbate layers at the electrode/electrolyte interfaces, Electrochem. Commun. 27 (2013) 42–45.
[33] S.H. Glarum, J.H. Marshall, An A-C Admittance study of the platinum/sulfuric acid interface, J. Electrochem. Soc. 126 (1979) 424.
[34] M. Schalenbach, Y.E. Durmus, H. Tempel, H. Kungl, R.A. Eichel, Double layer capacitances analysed with impedance spectroscopy and cyclic voltammetry: validity and limits of the constant phase element parameterization, Phys. Chem. Chem. Phys. 23 (2021) 21097–21105.
[35] M.H. Martin, A. Lasia, Influence of experimental factors on the constant phase element behavior of Pt electrodes, Electrochim. Acta 56 (2011) 8058–8068.
[36] P. Charoen-amornkitt, W. Pholauyphon, T. Suzuki, S. Tsushima, An approach to unify capacitance measurements of electric double layer capacitors using sinusoidal potential scan, J. Energy Storage 66 (2023) 107522.
[37] P. Córdoba-Torres, T.J. Mesquita, R.P Nogueira, Relationship between the origin of constant-phase element behavior in electrochemical impedance spectroscopy and electrode surface structure, J. Phys. Chem. C 119 (2015) 4136–4147.
[38] Z. Kerner, T. Pajkossy, Impedance of rough capacitive electrodes: the role of surface disorder, J. Electroanal. Chem. 448 (1998) 139–142.
[39] T. Pajkossy, T. Wandlowski, D.M. Kolb, Impedance aspects of anion adsorption on gold single crystal electrodes, J. Electroanal. Chem. 414 (1996) 209–220.
[40] B. Hirschorn, et al., Determination of effective capacitance and film thickness from constant-phase-element parameters, Electrochim. Acta 55 (2010) 6218–6227.
[41] V.M.W. Huang, V. Vivier, M.E. Orazem, N. Pébère, B. Tribollet, The apparent constant-phase-element behavior of a disk electrode with faradaic reactions: a global and local impedance analysis, J. Electrochem. Soc. 154 (2006) C99.
[42] T.I. Borisova, B.V Ershler, Determination of potentials of zero charge from double layer measurements, Zh. Fiz. Khim. 24 (1950) 337–344.
[43] J. Newman, Current distribution on a rotating disk below the limiting current, J. Electrochem. Soc. 113 (1966) 1235.
[44] J. Newman, Frequency dispersion in capacity measurements at a disk electrode, J. Electrochem. Soc. 117 (1970) 198.
[45] M.E. van der Geest, N.J. Dangerfield, D.A. Harrington, An ac voltammetry study of Pt oxide growth, J. Electroanal. Chem. 420 (1997) 89–100.
[46] T. Pajkossy, R. Jurczakowski, Electrochemical impedance spectroscopy in interfacial studies, Curr. Opin. Electrochem. 1 (2017) 53–58.
[47] O. Gharbi, M.T.T. Tran, B. Tribollet, M. Turmine, V. Vivier, Revisiting cyclic voltammetry and electrochemical impedance spectroscopy analysis for capacitance measurements, Electrochim. Acta 343 (2020) 136109.
[48] A.M. Bond, N.W. Duffy, G. Si-Xuan, J. Zhang, D. Elton, Changing the look of voltammetry, Anal. Chem. 77 (2005), 186 A-195 A.
[49] J.C. Myland, K.B. Oldham, Uncompensated resistance. 1. The effect of cell geometry, Anal. Chem. 72 (2000) 3972–3980.
[50] R.M. Souto, Electronic configurations in potentiostats for the correction of ohmic losses, Electroanalysis 6 (1994) 531–542.
[51] M. Schalenbach, Y.E. Durmus, H. Tempel, H. Kungl, R.A Eichel, A dynamic transmission line model to describe the potential dependence of double-layer capacitances in cyclic voltammetry, J. Phys. Chem. C 125 (2021) 27465–27471.
[52] A.C.H. Lazanas, M.I Prodromidis, Electrochemical impedance spectroscopy-A tutorial, ACS Meas. Sci. Au 3 (2023) 162–193.
[53] E. Sibert, R. Faure, R. Durand, High frequency impedance measurements on Pt (111) in sulphuric and perchloric acids, J. Electroanal. Chem. 515 (2001) 71–81.
[54] A. Lasia, The origin of the constant phase element, J. Phys. Chem. Lett. 13 (2022) 580–589.
[55] M.E. Orazem, B. Tribollet, Electrochemical Impedance Spectroscopy, John Wiley & Sons, Inc., 2008.
[56] M. Schalenbach, et al., Physicochemical mechanisms of the double-layer capacitance dispersion and dynamics: an impedance analysis, J. Phys. Chem. C 125 (2021) 5870–5879.
[57] G.J. Brug, A.L.G. van den Eeden, M. Sluyters-Rehbach, J.H Sluyters, The analysis of electrode impedances complicated by the presence of a constant phase element, J. Electroanal. Chem. Interfacial. Electrochem. 176 (1984) 275–295.
[58] C.H. Hsu, F. Mansfeld, Technical note: concerning the conversion of the constant phase element parameter Y0 into a capacitance, Corrosion 57 (2001) 747–748.
[59] M.W. Breiter, Impedance on platinum from voltammetry with superimposed alternating voltage, J. Electroanal. Chem. 7 (1964) 38–49.
[60] R. Rizo, et al., Investigating the presence of adsorbed species on Pt steps at low potentials, Nat. Commun. 13 (2022) 2550.
[61] D.A. Harrington, Ac voltammetry for measurement of surface kinetics, J. Electroanal. Chem. 355 (1993) 21–35.
[62] J. Clavilier, The role of anion on the electrochemical behaviour of a {111} platinum surface; an unusual splitting of the voltammogram in the hydrogen region, J. Electroanal. Chem. Interfacial Electrochem. 107 (1980) 211–216.
[63] P.J. Welford, B.A. Brookes, V. Climent, R.G. Compton, The hanging meniscus contact: geometry induced diffusional overpotential. The reduction of oxygen in dimethylsulphoxide at Au(111), J. Electroanal. Chem. 513 (2001) 8–15.
[64] P. Córdoba-Torres, et al., On the intrinsic coupling between constant-phase element parameters α and Q in electrochemical impedance spectroscopy, Electrochim. Acta 72 (2012) 172–178.
[65] C.L. Alexander, B. Tribollet, M.E. Orazem, Contribution of surface distributions to constant-phase-element (CPE) behavior: 1. Influence of roughness, Electrochim. Acta 173 (2015) 416–424.
[66] A.M. Bond, R.J. O'Halloran, I. Ruzic, D.E.A.C. Smith, Cyclic voltammetry: a digital simulation study of the slow scan limit condition for a reversible electrode process, J. Electroanal. Chem. Interfacial. Electrochem. 90 (1978) 381–388.
[67] P.C. Wayner, The effect of viscous shear on a meniscus in an electrochemical system, J. Electrochem. Soc. 119 (1972) 584.
[68] C. Costentin, J.M. Savéant, Ohmic drop correction in electrochemical techniques. Multiple potential step chronoamperometry at the test bench, Energy Storage Mater. 24 (2020) 1–3.
[69] I. Frateur, et al., Local electrochemical impedance spectroscopy: considerations about the cell geometry, Electrochim. Acta 53 (2008) 7386–7395.